NASA TECHNICAL NOTE

NASA TN D-2931

LUMINOUS EFFICIENCY OF AN ARTIFICIAL METEOR AT 11.9 KILOMETERS PER SECOND

by Wendell G. Ayers

Langley Research Center
Langley Station, Hampton, Va.

NATIONAL AERONAUTICS AND SPACE ADMINISTRATION • WASHINGTON, D. C. • AUGUST 1965

LUMINOUS EFFICIENCY OF AN ARTIFICIAL METEOR AT 11.9 KILOMETERS PER SECOND

By Wendell G. Ayers

Langley Research Center
Langley Station, Hampton, Va.

NATIONAL AERONAUTICS AND SPACE ADMINISTRATION

For sale by the Clearinghouse for Federal Scientific and Technical Information
Springfield, Virginia 22151 – Price $2.00

LUMINOUS EFFICIENCY OF AN ARTIFICIAL METEOR AT 11.9 KILOMETERS PER SECOND

By Wendell G. Ayers
Langley Research Center

SUMMARY

A brief description is given of the Trailblazer IIb artificial meteoroid experiment, which consisted of reentering a 2.2-gram stainless-steel pellet into the earth's atmosphere at a reentry velocity of 11.9 km/sec. The methods of obtaining optical data and the data reduction procedures are outlined. The efficiency with which the kinetic energy of the artificial meteoroid was converted into effective radiant energy in the spectral sensitivity range of a panchromatic photographic emulsion was calculated from the observational data to be 1.2×10^{-2}. This value for the panchromatic luminous efficiency factor was found to be in good agreement with values from a similar experiment. The effects of differences in the spectral sensitivity of different detectors on measurements of the luminous efficiency factor are discussed, and methods of correlating results from different detectors are presented.

INTRODUCTION

The efficiency with which kinetic energy of a meteoroid entering the earth's atmosphere is converted into radiant energy is one of the major unresolved problems of meteor physics. The efficiency of this energy conversion process in the visible portion of the spectrum is known as the luminous efficiency factor of a meteor. This is an important parameter in meteor theory; it is often used in the calculation of meteoroid masses from data acquired by optical observation of meteors. Until recently estimates of the luminous efficiency by different investigators have varied as much as two orders of magnitude from 2×10^{-2} to 2×10^{-4}. (See ref. 1.)

The Trailblazer IIb flight test described herein was the second experiment of a type specifically designed to measure the luminous efficiency factor of an artificial meteor. A multistage solid-fuel rocket vehicle was used to reenter a small pellet of known mass and composition into the earth's atmosphere within the altitude and velocity ranges of a natural meteor. Natural meteors appear in the altitude range of 60 to 130 kilometers and at velocities between 8 and 72 km/sec. Photographs were made of the luminous reentry to provide the data necessary to compute the luminous efficiency factor.

The purpose of this paper is to give a brief description of the experiment, an analysis of the optical data used to obtain a value for the luminous efficiency factor, and a comparison of the results with previous experimental values and theoretical estimates for the luminous efficiency of natural meteors.

SYMBOLS

C	color index
D	optical density
d	distance, km
H	irradiance, ergs/cm^2-sec
M	absolute meteor magnitude
M_o	luminosity factor
m	mass, g
P	radiant power, ergs/sec
P_o	radiant power of a zero-magnitude meteor, ergs/sec
S	relative spectral sensitivity function
t	time, sec
V	velocity, cm/sec
ρ_m	meteoroid density, g/cm^3
τ	luminous efficiency factor
τ_o	luminosity coefficient, sec/cm
τ_o'	luminosity coefficient, sec^4/g-cm^3

Subscripts:

b	photographic, blue sensitive
p	photographic, panchromatic
s	dependent on characteristics of detector

v	visual
λ	wavelength

THEORETICAL CONSIDERATIONS

Basic meteor theory (ref. 2) defines a dimensionless luminous efficiency factor τ for a meteor by assuming that the instantaneous value of the radiant power P produced by the meteor is proportional to the rate of loss of kinetic energy from the meteoroid by ablation:

$$P = \frac{1}{2} \tau \left(-\frac{dm}{dt}\right) V^2 \tag{1}$$

Equation (1) is a general statement about the radiation from a meteor over the whole spectrum, but practical devices for detecting and measuring this radiation are limited in their response to a relatively narrow spectral band of radiation.

Detector Effects

Equation (1) may be modified to take into account such effects as atmospheric absorption and the response of the detector. If this is done, the relationship between the "effective" radiant power and the rate of loss of kinetic energy by ablation can be written as

$$P_s = \frac{1}{2} \tau_s \left(-\frac{dm}{dt}\right) V^2 \tag{2}$$

The subscript s in equation (2) is a general term indicating that P_s and consequently τ_s are detector dependent. The three detection systems considered in this report will be the eye, a blue sensitive photographic system, and a photographic system using panchromatic emulsions. Typical relative sensitivity curves for these detectors are shown in figure 1. Figure 1(b), from reference 3, represents the response of the dark adapted eye. The two photographic curves (fig. 1(a), from ref. 4, and fig. 1(c), from ref. 5) include the general absorption effects of a system containing refractive optical components. The general term s in equation (2) will be replaced by the subscripts v, b, or p in the subsequent discussion, depending on the type of detector under consideration. Since the radiation from meteors is predominately bright-line radiation (ref. 1), considerable variation between values for P_s from detectors with different spectral response characteristics might be expected even if the bandwidths of the detectors are nearly the same.

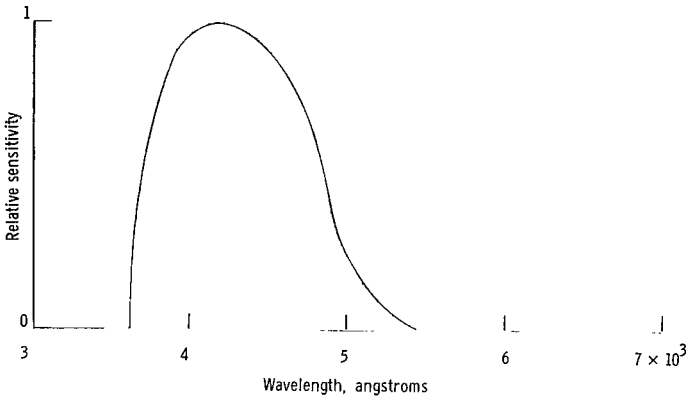

(a) Blue sensitive photographic emulsion with refractor optics.

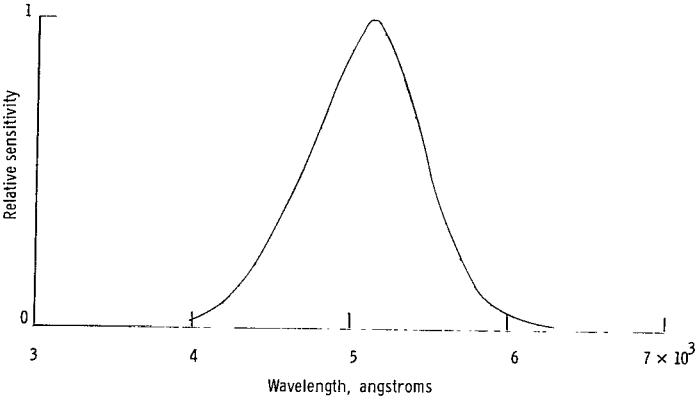

(b) Dark adapted human eye.

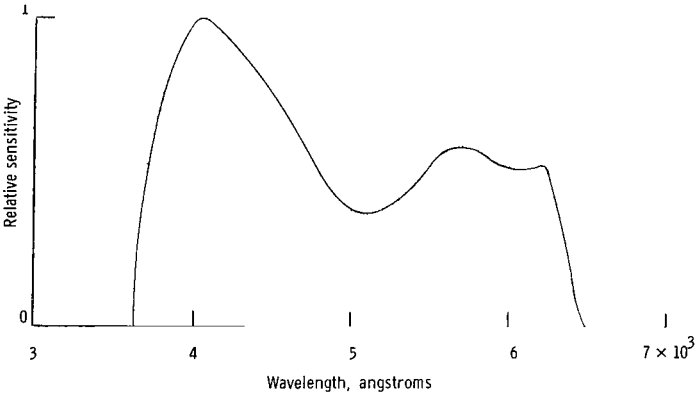

(c) Panchromatic photographic emulsion with refractor optics.

Figure 1.- Typical spectral sensitivity curves for three detectors.

Effects of Velocity on τ_s

Öpik, as early as 1933 (see ref. 6), considered the problem of visible radiation from meteors. He concluded that the primary source of radiation from most meteors is atomic emission from the vaporized meteor atoms after collisions with air molecules at the velocity of the meteoroid. Using laboratory experiment and classical physical reasoning he was able to estimate the amount of visible radiation produced by such collisions. Öpik's estimates were extensively used by meteor astronomers who applied his values for the luminous efficiency factor to photographic meteor data and were able to estimate the mass of meteoroids producing a given amount of light at a particular velocity. A smooth curve representation of Öpik's 1933 data for bright meteors is shown by curve I in figure 2(a).

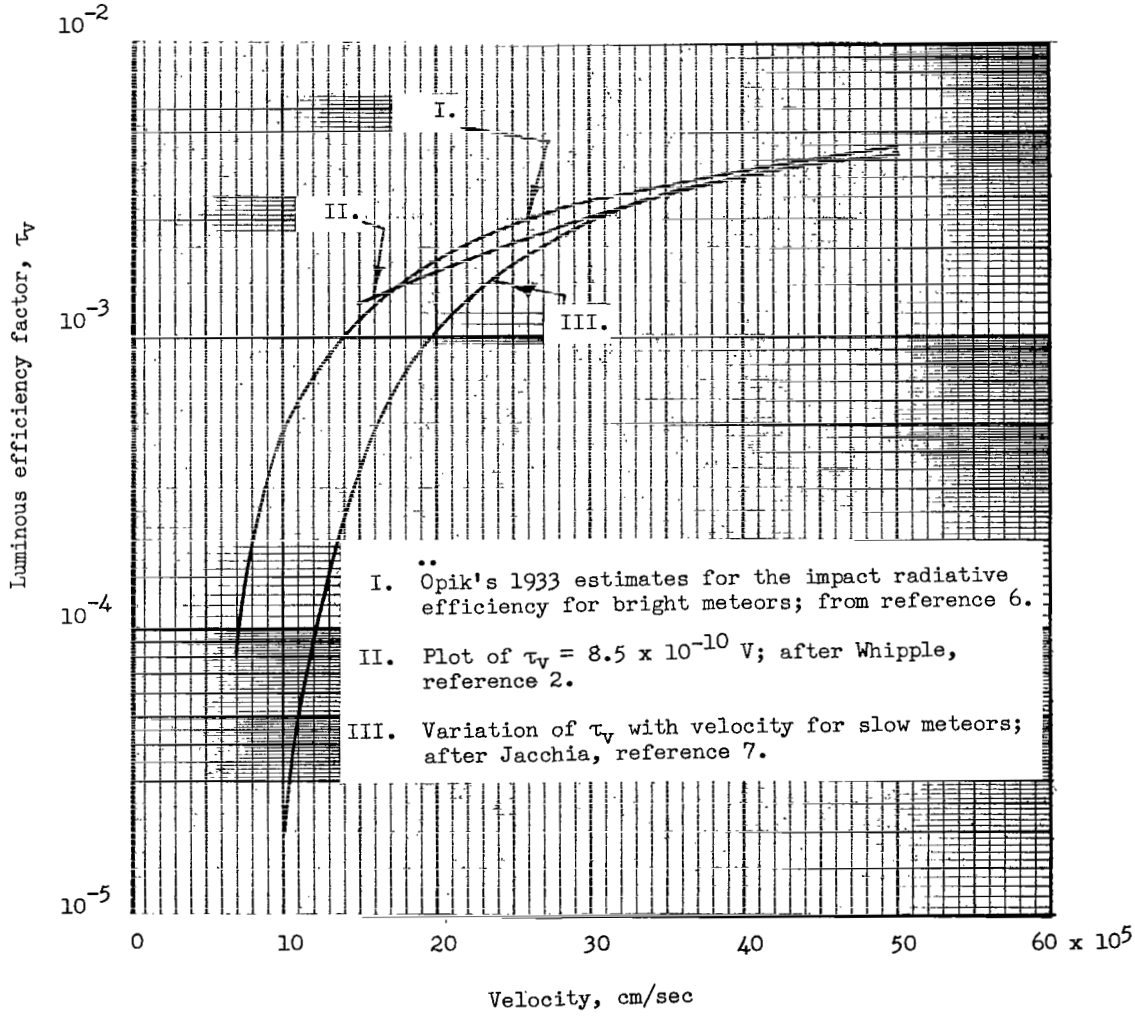

(a) Based on Öpik's 1933 data.

Figure 2.- Values for the luminous efficiency factor.

Jacchia and Whipple (ref. 2) noted that Öpik's data could be represented by a relation of the form

$$\tau_V = \tau_{O,V} V \qquad \text{for} \quad V > 15 \text{ km/sec} \tag{3}$$

where the luminosity coefficient $\tau_{O,V}$ has a value of 8.5×10^{-10} sec/cm. Curve II in figure 2(a) is a plot of equation (3) with this value of $\tau_{O,V}$.

Jacchia, in 1949 (see ref. 7), was able to calculate the variation of τ_V with velocity from photographic observations of 10 natural meteors with velocities less than 45 km/sec. Assuming Whipple's value of $\tau_{O,V}$ (and consequently Öpik's values of τ_V) to be correct for velocities greater than 30 km/sec, Jacchia calculated the relative variation of τ_V with velocity and reported it in terms of the luminosity factor M_O, a quantity related to the luminosity coefficient $\tau_{O,V}$ by the equation

$$M_O = -2.5 \log \frac{\tau_{O,V}}{2P_{O,V}} \tag{4}$$

Equation (4) is derived in appendix A which contains a general discussion of some of the quantities related to the luminous efficiency factor which have appeared in the literature. Jacchia's values for M_O are converted herein to values for τ_V and are represented by curve III in figure 2(a).

In 1958 (ref. 3), Öpik published the results of further study of the meteor problem. In this work he discusses three sources of meteor radiation and provides tabulated data and formulas to compute the efficiency of each of these processes for meteors of different types. The visual luminous efficiency factor τ_V is according to Öpik the sum of three factors: (1) impact radiative efficiency, or the efficiency with which visible radiation is produced by impacts between meteor atoms and air particles at the velocity of the meteor; (2) temperature radiative efficiency, or the efficiency with which visible radiation is produced by thermal impacts between particles in the meteor wake; and (3) blackbody radiative efficiency, or the efficiency with which visible radiation is produced by continuous radiation from the heated surface of the meteoroid. Of these factors, the impact efficiency is the greatest except for the case of large meteoroids at low velocities.

Figure 2(b) is a plot of the efficiency factors for a 2-gram compact iron meteoroid based on Öpik's 1958 data. Curves I, II, and III are the blackbody, temperature, and impact radiative efficiencies, respectively, and curve IV is the sum of the three.

The major difference between Öpik's 1933 and 1958 estimates is the dependence of τ_V on velocity. According to the 1933 data, τ_V increases linearly with velocity for velocities greater than 15 km/sec. However, the 1958 data show that τ_V is almost independent of velocity at the higher velocities and varies as some negative power of the velocity in the intermediate range.

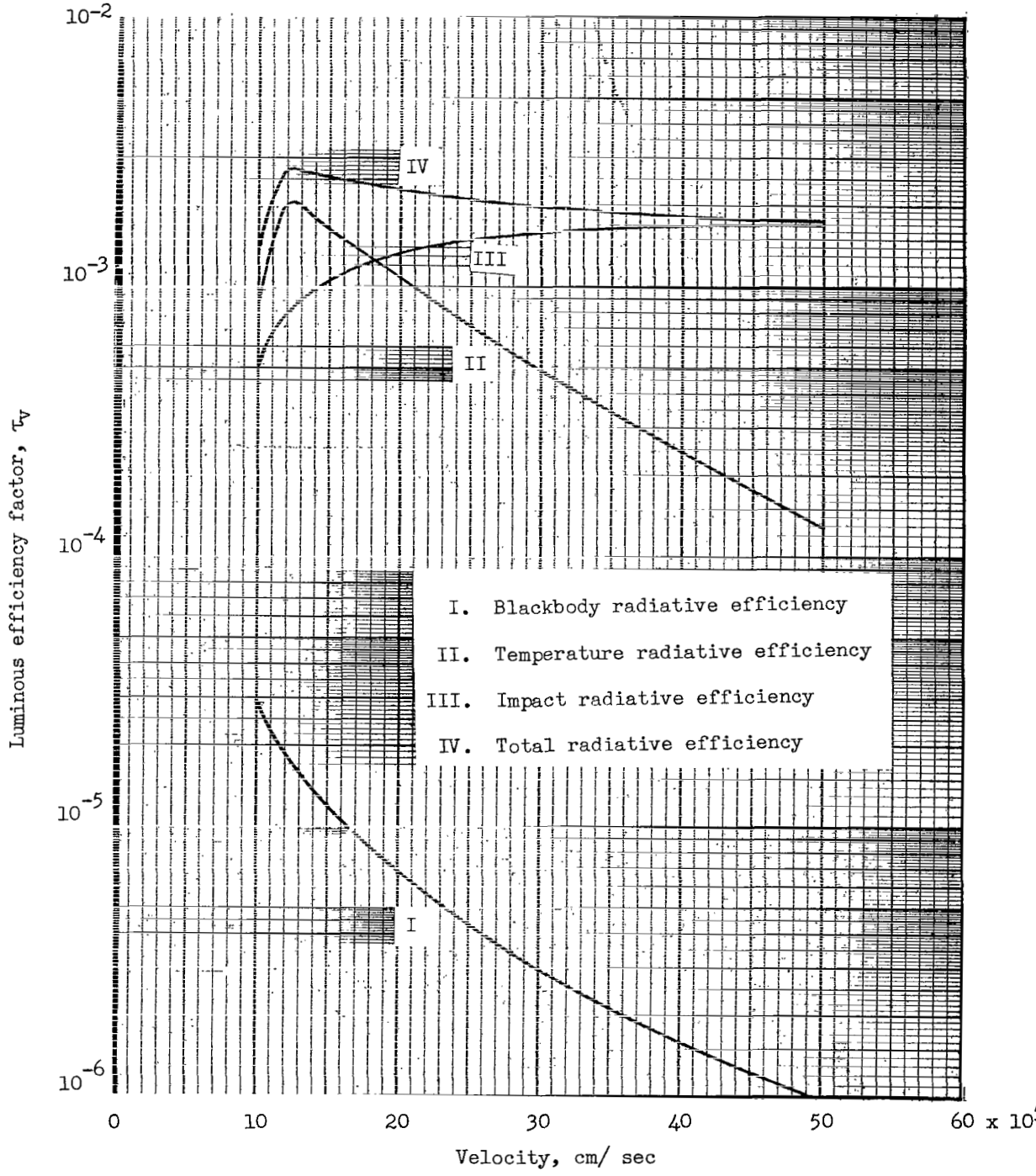

(b) Calculated from Öpik's 1958 data for 2-gram compact iron meteoroid.

Figure 2.- Continued.

Verniani (ref. 8) has recently published the results obtained from 400 photographic (blue sensitive) meteors. He found that the observational data could best be represented by an equation of the form

$$\tau_b = \tau_{o,b} v^n \tag{5}$$

with $n = 1.0 \pm 0.15$. Verniani's results are more consistent with the 1933 data of Öpik than his 1958 data.

Effects of Materials on τ_s

The quantity and spectral distribution of the radiation produced by a meteor depend upon the chemical composition of the meteoroid as well as its velocity. The chemical composition of meteorites has been well documented (see ref. 9), but it is now believed that the great majority of meteors are produced by objects with origins different from those of meteorites (ref. 1, pp. 169-171). Little is known about the chemical composition of the most common meteoroid - the cometary meteoroid or "dust ball."

Öpik, in reference 3, treats three types of meteoroids: compact iron, compact stone, and dust balls made up of an aggregate of stone "grains." Figure 2(c) is a plot of the luminous efficiency factor for a 2-gram meteoroid of each of these classes and is based on data taken from reference 3. It is evident from the figure that the visual luminous efficiency for compact stone is calculated to be greater than that of iron at the lower velocities. Spectra from low-velocity meteors show that most of the radiation detected by blue sensitive emulsions arises from iron line emission (ref. 10). The observational evidence would lead one to suspect that stone would have a lower photographic efficiency than iron since meteorite stone contains only about 15 percent iron compared with 90 percent iron for iron-nickle meteorites.

Experimental Determination of τ_s

One method of experimentally determining values for τ_s, and the approach taken for this experiment, is to reenter particles of known mass and chemical composition into the earth's atmosphere at meteor heights and velocities. The velocity and position of reentry and the radiation from the artificial meteor can be measured with ground-based detectors. Now, equation (2) can be written in the following integral form:

$$\int_{m_2}^{m_1} dm = 2 \int_{t_1}^{t_2} \frac{P_s}{\tau_s v^2} dt \tag{6}$$

where the quantities on the right of the equation, with the exception of τ_s, are measurable. Equation (6) can be solved for τ_s in terms of the measured quantities if some assumptions are made about the limits on the integral of the left and about the functional relationship between τ_s and the variable of integration.

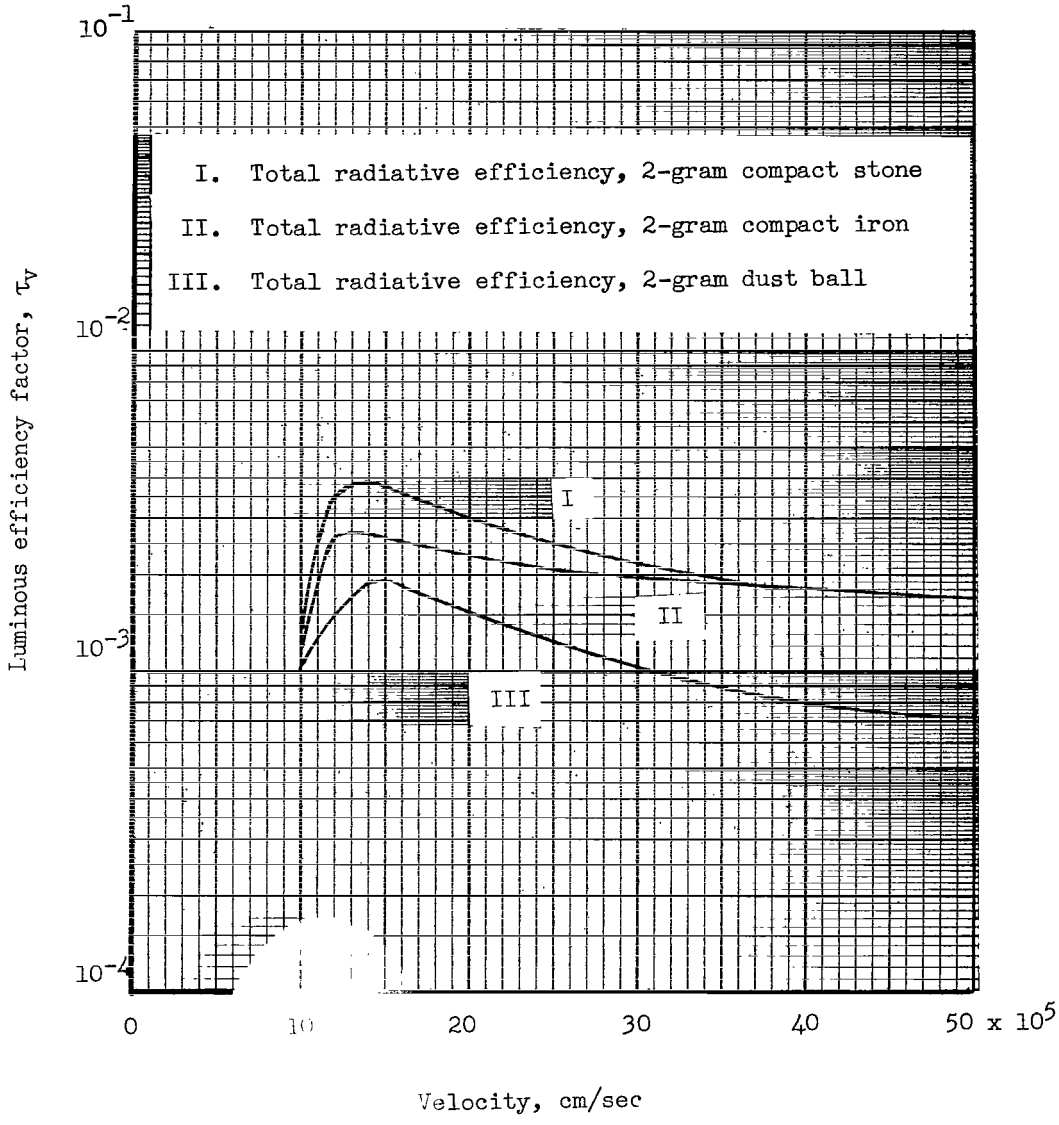

(c) Calculated from Öpik's 1958 data for three types of meteoroids.

Figure 2.- Concluded.

DESCRIPTION OF THE EXPERIMENT

The Trailblazer IIb experiment consisted of reentering a particle of known mass, chemical composition, and physical dimensions into the earth's atmosphere at meteor heights with a velocity comparable to that of a slow natural meteor. The luminous reentry was photographed from several ground stations, and the photographs were analyzed to obtain the altitude and range of the artificial meteor, the reentry velocity, and the photographic intensity of the radiation. Since the initial mass of the meteoroid was known, it was possible to compute the panchromatic luminous efficiency factor τ_{pan} of the artificial meteor from the observed quantities.

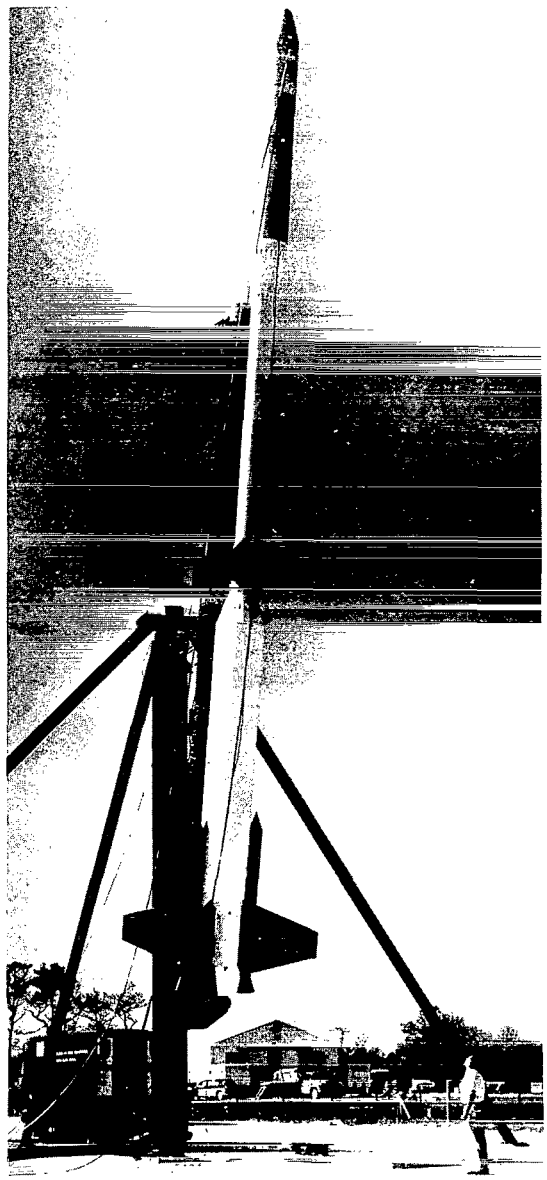

L-62-4432

Figure 3.- Trailblazer IIb vehicle in launch position.

The test vehicle was a six-stage unguided solid-fuel system. A photograph of the vehicle on the launch pad is shown in figure 3. The first two stages of the Trailblazer IIb were used to obtain the desired apogee. The remaining stages, shown in figure 4, are called the velocity package. These stages faced in a rearward direction at launch and were fired in sequence, downward toward the earth, from a point near apogee. The four stages of the velocity package accelerated a small (2.2 grams) stainless-steel pellet to a reentry velocity of 11.9 km/sec. Figure 5 is a composite photograph made of a similar projectile before and after the ground firing of a shaped-charge accelerator. It was an accelerator of the same type that was used as the last stage of the Trailblazer IIb. The test vehicle was designed to produce a reentry near the launch site and within the data acquisition range of the ground-based equipment. A detailed description of the vehicle and its performance can be found in reference 11.

Ground-based radar near the launch site at the NASA Wallops Station tracked the vehicle through reentry of the fifth stage. Photographs of the reentry of the artificial meteor were obtained from all of the optical stations. Figure 6 shows the nominal trajectory, the radar track, and that portion of the

trajectory recorded by the cameras. Figure 7 gives the geographic location of optical stations and the nominal flight path of the vehicle.

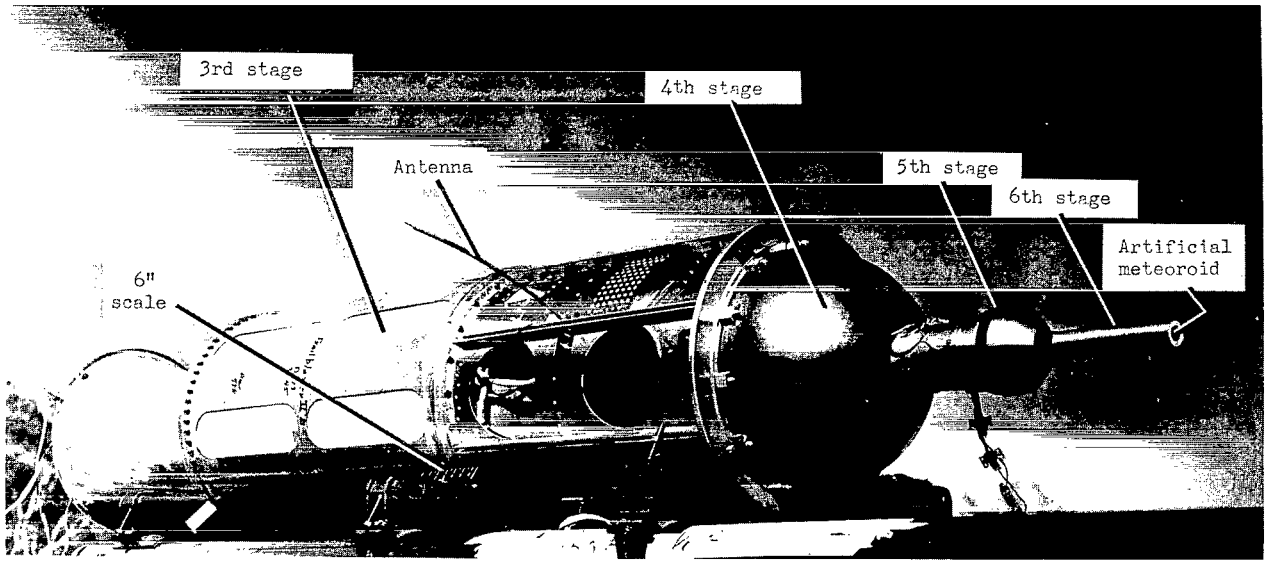

Figure 4.- The last four stages of the Trailblazer IIb. L-62-4040.1

Photographs of the reentry were obtained from several cameras at each of the optical stations. These cameras included Super-Schmidt meteor cameras operated by MIT - Lincoln Laboratory and ballistic and modified aerial cameras operated by the NASA Langley Research Center. Several of the cameras were equipped with occulting shutters for velocity measurements; several were equipped with spectral gratings; the rest were operated with an uninterrupted time exposure to yield streak photographs. Most of the ballistic and aerial cameras were equipped with films or plates with panchromatic emulsions. The results reported herein are based on photometry from the undispersed panchromatic records, since they were the only Langley records yielding data of sufficient quality. A typical panchromatic photograph of the meteor taken from the Coquina Beach, N.C., site is shown in figure 8. The meteor in figure 8 appears in the constellation Cygnus near the γ star of that group. The brightness of the meteor, as it appears in the photograph, is near that of a seventh magnitude star. However, the angular velocity of the meteor about the optical center of the camera was much greater than that of the stars. If the angular velocity of the meteor had been the same as that of the stars, the meteor would have an apparent photographic brightness greater than that of the γ star.

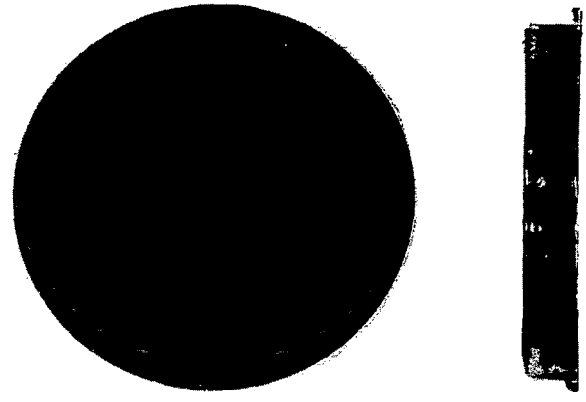

(a) Projectile before ground firing of shaped-charge accelerator.

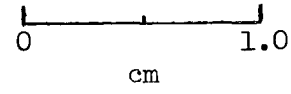

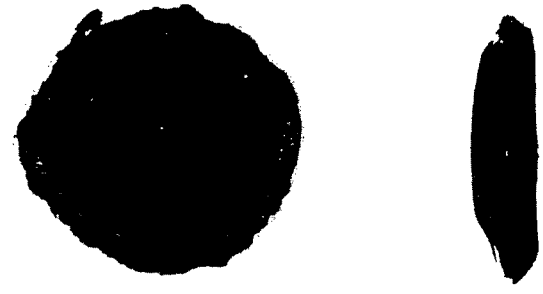

(b) Projectile recovered from ground firing of shaped-charge accelerator.

L-65-107

Figure 5.- Composite photograph of the type of projectile used in the Trailblazer IIb experiment.

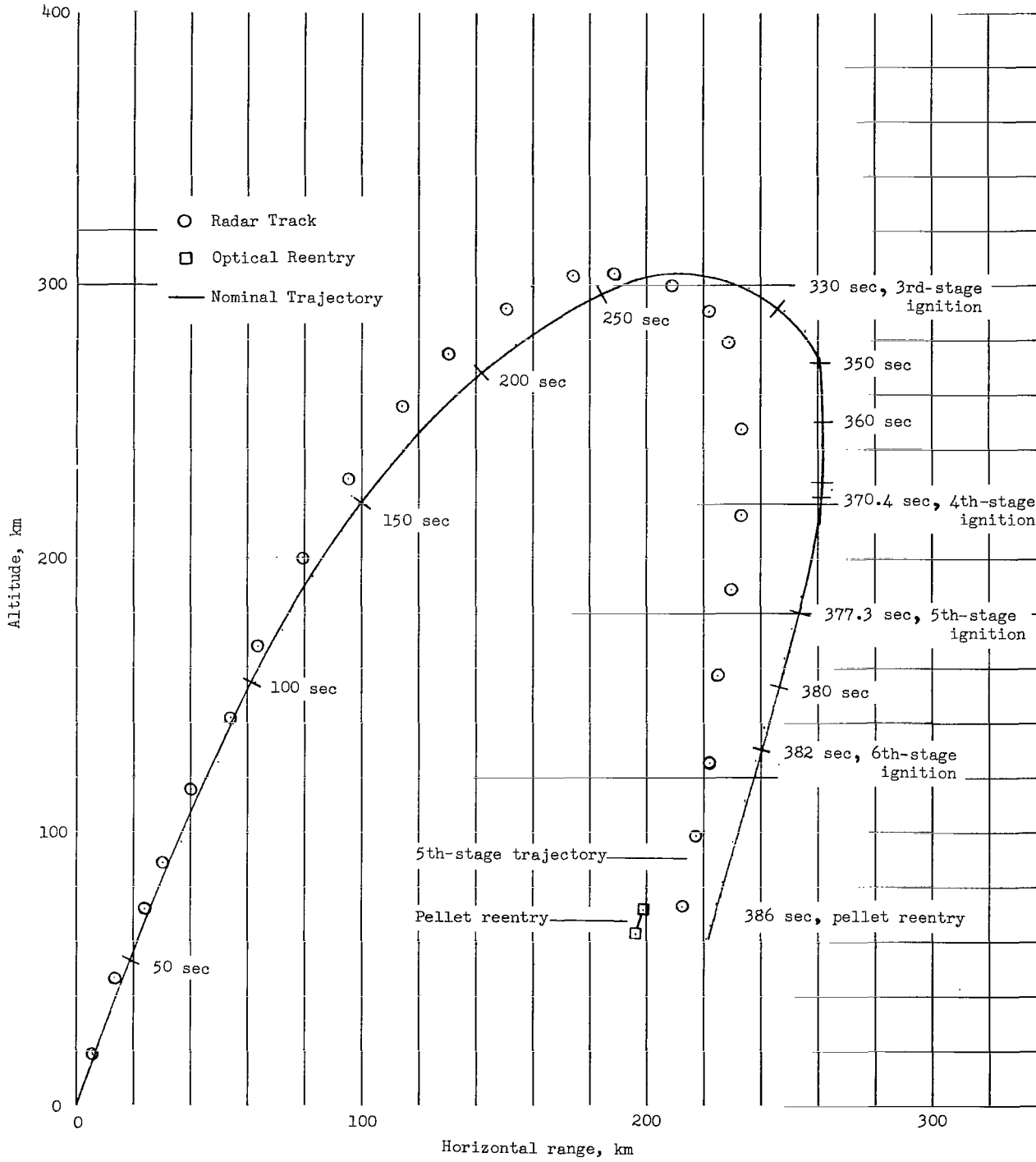

Figure 6.- Trailblazer IIb trajectory.

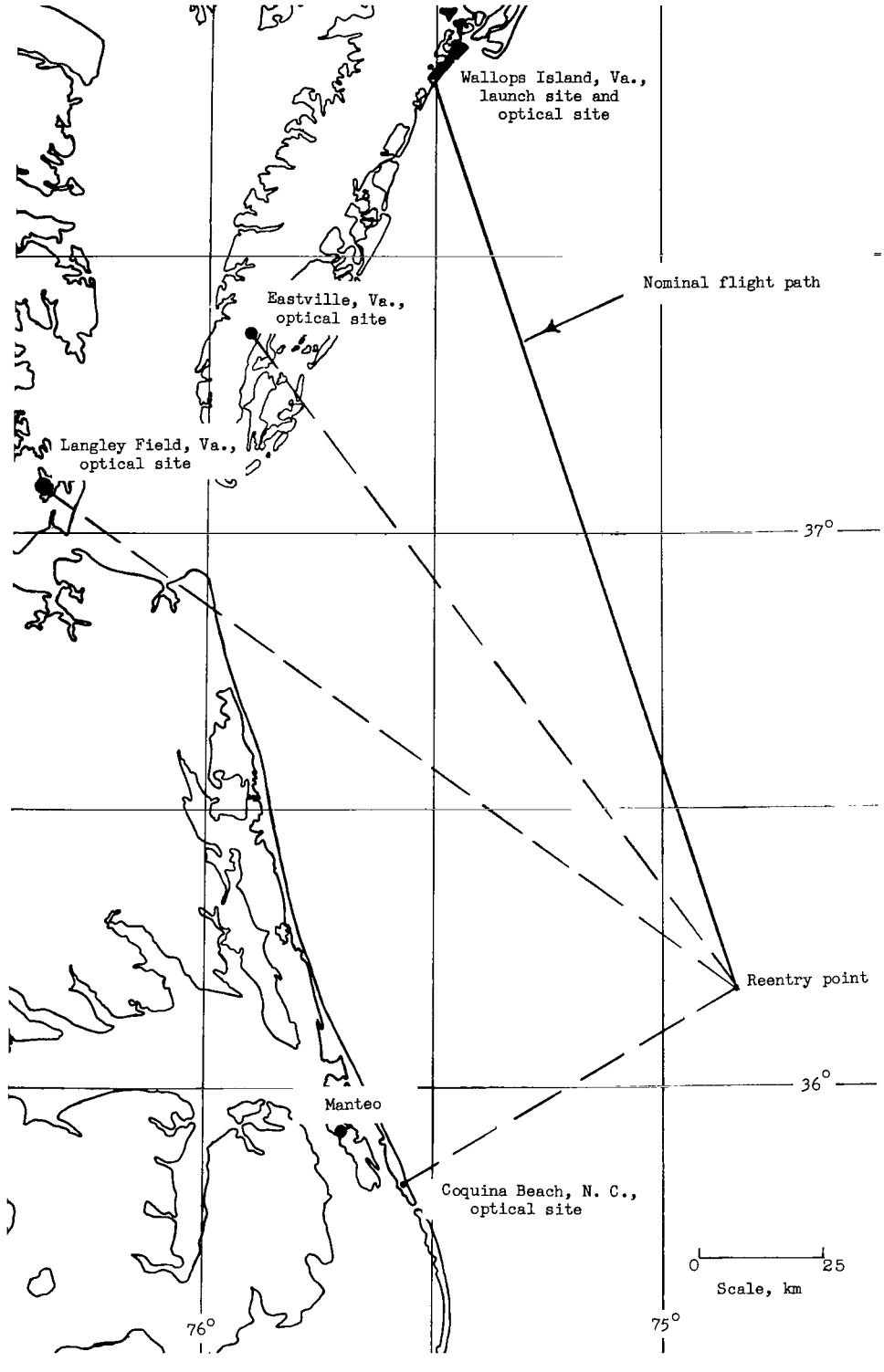

Figure 7.- Geographic location of Trailblazer IIb pellet reentry and optical stations.

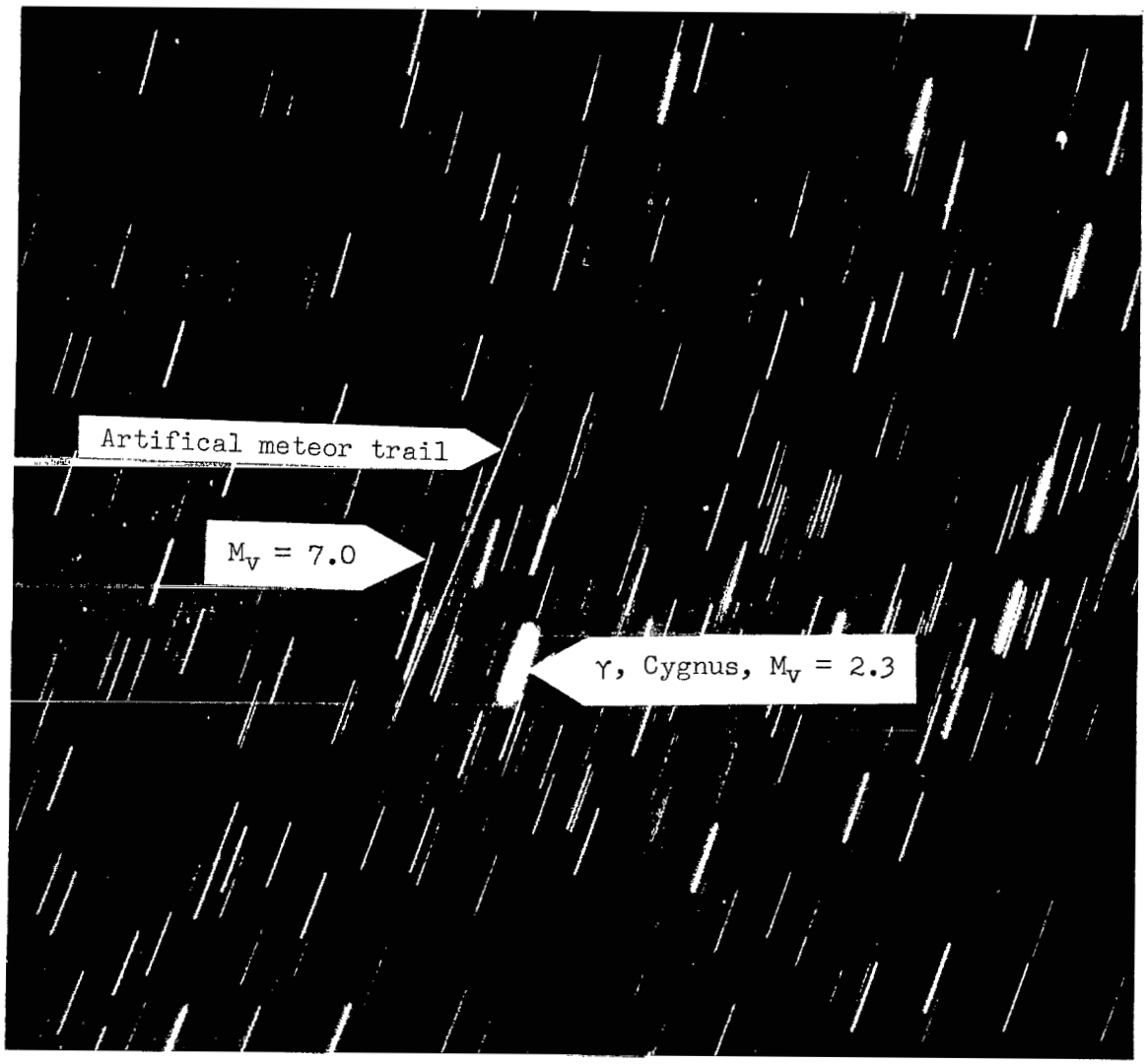

L-65-108

Figure 8.- Enlarged photograph of the Trailblazer IIb artificial meteor taken from Coquina Beach, N.C.

ANALYSIS OF THE OPTICAL DATA

The ballistics data reduction followed a procedure based on a program developed to determine precise orbits of natural meteors as outlined in reference 12. The determination of meteor position from photographs taken at two stations is based on the difference in the position of the meteor against the stellar background as photographed from each station.

The velocity and deceleration of the meteor can be determined if at least one of the photographs is made with a camera equipped with an occulting shutter.

A camera with such a shutter photographs the meteor as a series of dashes rather than a continuous streak - each dash corresponding to a known time increment. In the data reduction process, the observed distances d along the meteor trails are fitted by least squares to an equation of the form

$$d = a + bt + ce^{kt} \tag{7}$$

where a, b, c, and k are constants to be determined. The first differentiation of this equation gives the velocity as a function of time. A curve showing the velocity plotted against time for the artificial meteor is given in figure 9.

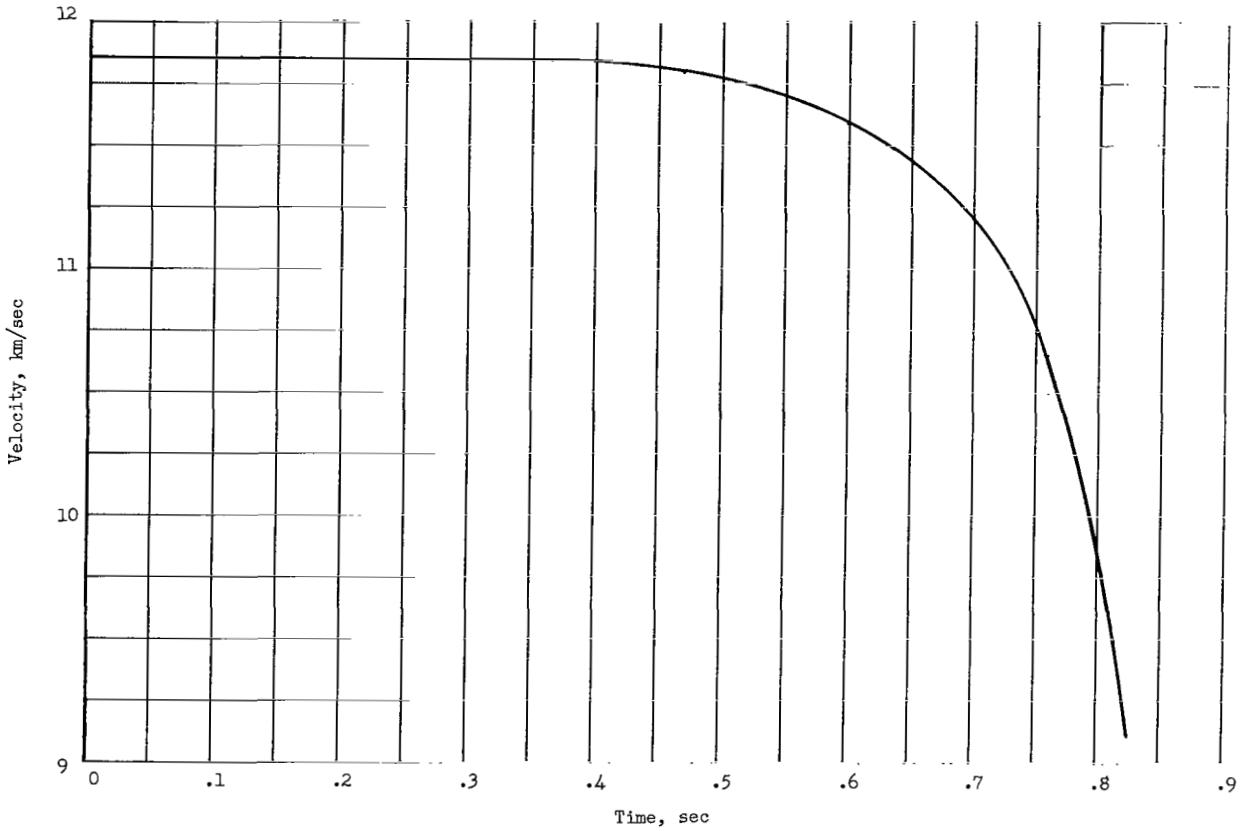

Figure 9.- Reentry velocity of the Trailblazer IIb artificial meteoroid.

A photograph from each of three stations was selected for photometry. Each of these photographs was paired with a Super-Schmidt photograph taken from Eastville, Va., to obtain the necessary ballistics data. The velocity data were obtained from the Eastville record. Trajectory data from each of the stations are included in table I.

TABLE I.- BALLISTICS DATA FOR TRAILBLAZER IIb

ARTIFICIAL METEOR

Station	Beginning height, km	Terminal height, km	Beginning range, km	Terminal range, km
Wallops	73.7	67.5	211.0	206.7
Eastville	74.9	66.9	184.7	179.2
Langley	73.9	66.6	198.8	194.3
Coquina	74.1	66.7	117.8	113.8

TABLE II.- PHOTOMETRIC DATA FOR TRAILBLAZER IIb

ARTIFICIAL METEOR

Station	Seeing condition	Camera	Focal length, mm	f-number	Detector spectral bandwidth, Å	Occulting shutter
Wallops	Scattered haze	Modified aerial K-24	270	2.5	3600 to 6400	Yes
Langley	Haze; sky light from city	Ballistic	304	2.6	3600 to 7000	No
Coquina	Excellent	Ballistic	304	2.6	3600 to 6400	No

A time history of the panchromatic luminous power of the meteor was obtained from the three panchromatic records. (Data on the cameras and photographic emulsions are given in table II.) The photometry of these records was based on the methods of meteor photometry outlined in reference 7. A recording microphotometer was used to measure density profiles of the trail and nearby star images. A calibration curve was formed from the measured densities of the comparison stars and their visual magnitudes from the Henry Draper Catalog (ref. 13). The magnitudes were corrected according to the star positions on the photographic plate. It was found experimentally (see appendix B) that the panchromatic magnitudes of most stars are close approximations to their visual magnitudes. A value for the magnitude of points along the meteor trail was established by comparison of the density measurements of the trail with the calibration curve. The magnitude values that were obtained from each of the records were then converted to absolute meteor magnitudes as defined in appendix A. The conversion from the uncorrected magnitudes M' as determined by the calibration curve to an absolute meteor magnitude M_p may be represented by the sum:

$$M_p = M' + \Delta M_V + \Delta M_R + \Delta M_Z + \Delta M_t + \Delta M_r \qquad (8)$$

The quantity ΔM_V represents a correction for the difference in the trailing velocity of the meteor image and the trailing velocity of the star image on the photographic plate. The quantity ΔM_R represents a correction for the difference between the range of the meteor and 100 kilometers. The quantity ΔM_Z represents a correction for the zenith angle. This correction is zero if the comparison stars are chosen from the meteor photograph and sufficiently near the meteor. The correction ΔM_t represents a correction applied to photographs made with an occulting shutter. It is a correction for the difference in the effective exposure time between the meteor and the stars. A correction for reciprocity failure ΔM_r of the photographic emulsion has also been taken into account. According to information furnished by the film manufacturer, this correction should be quite small for the emulsions used and consequently has been taken to be zero. The velocity correction ΔM_V is the largest correction. This correction, in some instances, amounted to minus eight magnitudes.

The light curve for the artificial meteor is shown in figure 10. The symbols indicate the results from the different records. The agreement between the results obtained from each of the stations is generally very good despite the differences in cameras, emulsions, and seeing conditions for each station. The shape of the Trailblazer IIb light curve is similar to the light curve from a previous experiment which was designated the Trailblazer Ig. Results from the Trailblazer Ig experiment have been reported by McCrosky and Soberman in reference 10 and Jewell and Wineman in reference 14. McCrosky and Soberman noted that the dip in the Trailblazer Ig light curve is "compared to natural meteors . . . a most unusual event." The reoccurrence of this dip in the light curve is an indication that the two artificial meteoroids went through similar modes of ablation.

McCrosky and Soberman discuss the possible modes of ablation in some detail using the dip in the light curve as part of their analysis. They came to the conclusion that the first half of the mass is lost as liquid droplets by spraying and that the duration of the dip in the light curve corresponds to the time to liquefy the remaining mass which will then break up into small droplets on the order of 2 millimeters in diameter. Consequently, the terminal mass of the meteoroid is quite small. The microphotometer traces of the photographic records of the Trailblazer IIb experiment indicate a broadening of the image near the end of the trail and rapid termination of the visible streak. Since a spray of liquid droplets would produce such an event, this can be taken as supporting evidence that the terminal mass of the meteoroid is indeed small.

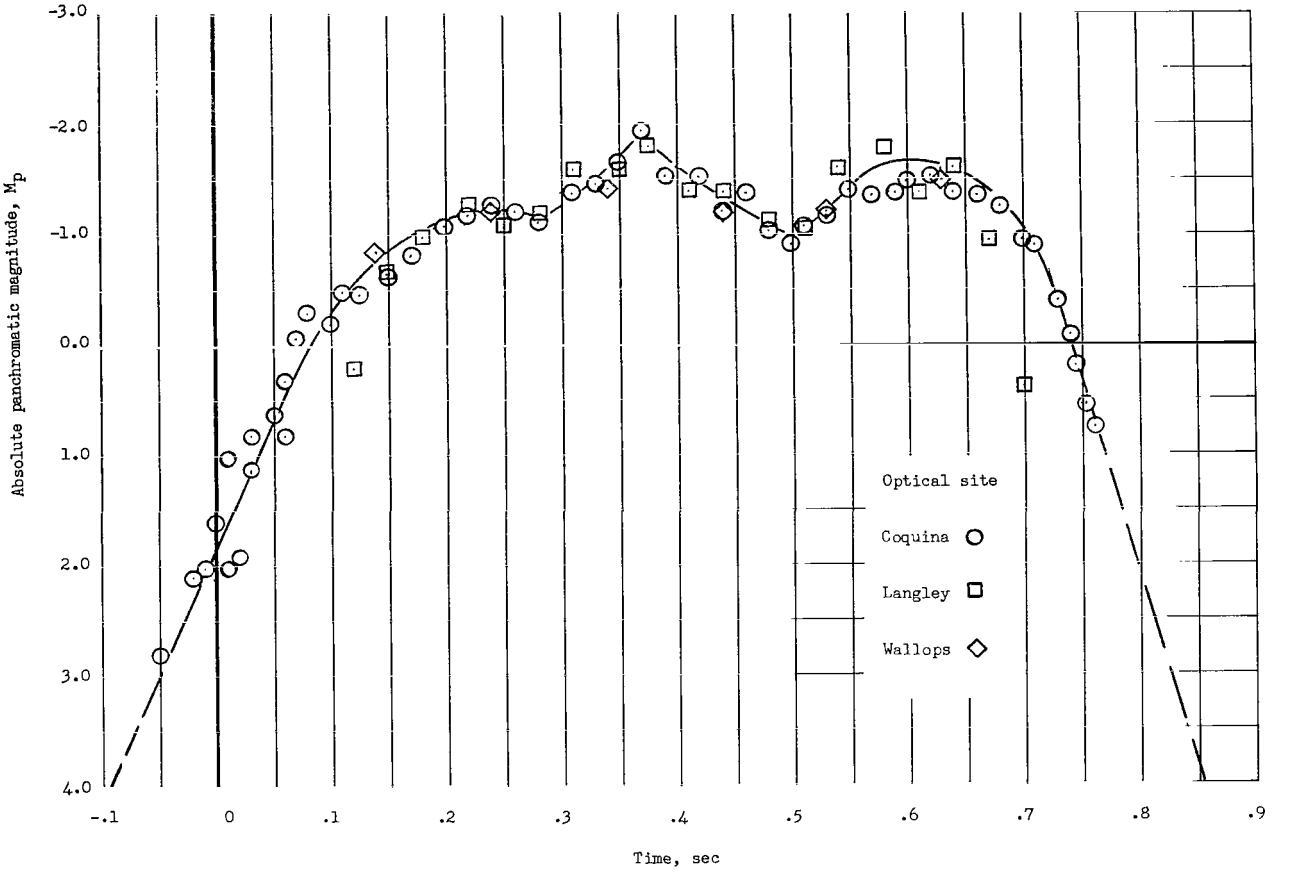

Figure 10.- Panchromatic light curve of the Trailblazer IIb artificial meteor.

RESULTS FROM THE FLIGHT TEST

The Trailblazer IIb flight test yielded the data needed to compute values for the panchromatic luminosity coefficient and the panchromatic luminous efficiency factor for the artificial meteor. Equation (6) was used as the basis of these computations.

Equation (6) may be written in terms of a panchromatic detector as

$$\int_{m_2}^{m_1} dm = \int_{t_1}^{t_2} \frac{P_p}{\tau_p V^2} dt \tag{9}$$

The quantity P_p can be expressed in terms of absolute panchromatic magnitude M_p by noting that

$$P_p = P_{o,p}10^{-0.4M_p} \tag{10}$$

from equation (A1) in appendix A.

A quantity related to τ_p can be removed from the integral by assuming that the panchromatic luminous efficiency factor is a linear function of velocity over the velocity range of the meteor and can be represented by an equation of the form

$$\tau_p = \tau_{o,p}V \tag{11}$$

The luminosity coefficient $\tau'_{o,p}$, a quantity closely related to the observational data, may be computed by noting that

$$\tau_{o,p} = P_{o,p}\tau'_{o,p} \tag{12}$$

from equation (A7) in appendix A.

By substituting equations (10), (11), and (12) into equation (9), the expression for the luminosity coefficient becomes

$$\tau'_{o,p} = 2\left(\frac{\int_{t_1}^{t_2} \frac{10^{-0.4M_p}}{V^3}\,dt}{\int_{m_2}^{m_1} dm}\right) \tag{13}$$

The integral in the numerator of the right-hand side of equation (13) was evaluated for the artificial meteor by a numerical integration of the observed quantities. In carrying out the integration, it was assumed that the light curve drops linearly toward $+\infty$ at each end as shown in figure 10. The integral in the denominator was evaluated by assuming that the initial mass was 2.2 grams and the terminal mass of the meteoroid was negligibly small. The results of the computation give

$$\tau'_{o,p} = 1.3 \times 10^{-18}\ \text{sec}^4/\text{g-cm}^3$$

Substituting this value for $\tau'_{o,p}$ and the value for $P_{o,p}$ of 7.96×10^9 ergs/sec, from equation (A2c) of appendix A, into equation (12) gives

$$\tau_{o,p} = 1.0 \times 10^{-8} \text{ sec/cm}$$

Equation (11) was then used to calculate the panchromatic luminous efficiency factor

$$\tau_p = 1.2 \times 10^{-2}$$

for the stainless-steel meteoroid at a velocity of 11.9 km/sec.

Stainless steel was chosen for the experiment because of mechanical properties which made the firing of a solid pellet by the shaped-charge-accelerator technique possible. A chemical composition of 70 percent iron, 19 percent chromium, and 9 percent nickle is not characteristic of meteoric iron nor the metallic content of stony meteorites. The experimental values presented herein must therefore be regarded as valid for one material within a narrow velocity range.

DISCUSSION OF ERRORS

It is a difficult task to assign an index of precision to the numerical results from an experiment of this nature. The problem of determining the luminous efficiency from ground-based observations cannot be solved without simplifying assumptions. Since the accuracy of the final results depends upon these assumptions, the precision of the measurements leading to the results is estimated as follows:

(1) The mass of the artificial meteoroid was determined from static firings of shaped-charge accelerators of the type used in this experiment. This was done at the Air Force Cambridge Research Laboratory where this type of accelerator was developed. From 11 ground tests it was found that the firing of the shaped charge reduced the 5.8-gram cylindrical projectile to a pellet with a mass of 2.2 grams ±0.1 gram of approximately the same shape as the original disk. (See fig. 5.)

(2) The agreement of the ballistics data from different optical records may be taken as an index of the precision of the data. Ranges and heights from the different records agreed within 0.10 kilometer or better and velocity measurement agreed within 0.20 km/sec.

(3) The determination of the intensity of the meteor was the least accurate measurement. The scatter in the points along the light curve (fig. 10) is a measure of the uncertainty in the light data. The photometric data from each of the three stations do not deviate more than 0.2 magnitude from the mean over most of the light curve.

The estimated errors in the measured quantities as described in this section lead to a relative error of about 0.24 in the value for τ_p that is given in the preceding section.

COMPARISON OF TEST RESULTS WITH OTHER DATA

A comparison of the value for the luminous efficiency factor obtained from this experiment with previous values is not a straightforward process. The difficulty lies in the many forms in which the data have been presented. Each author has presented his findings in a form that best suits the problem at hand and not necessarily in a form that can readily be compared with other results.

For the purpose of comparison, the values reported in the different references have, by the methods of appendix A, been converted to values for the luminosity coefficient $\tau_{o,s}$.

The luminous efficiency factors ($\tau_s = \tau_{o,s}V$) from the Trailblazer IIb and Ig experiments and from the natural meteor data are shown in figure 11. The symbols on the curves indicate the velocity at which the value of $\tau_{o,s}$ was calculated from the observational data.

Jewell and Wineman report a value for $\tau_{o,v}$ of 1.02×10^{-9} sec/cm for the Trailblazer Ig artificial meteoroid - a stainless-steel pellet identical in design to the Trailblazer IIb artificial meteoroid at a velocity of 9.8 km/sec. This value was based on panchromatic data, but was converted to a visual scale by using a color index of 1.65 (ref. 14). A value for $\tau_{o,p}$ of 7×10^{-9} sec/cm has been calculated from Jewell and Wineman's data by removing the color index conversion factor from their calculations. No estimate of error was made by Jewell and Wineman.

McCrosky and Soberman (ref. 10) report a value of $\tau'_{o,b}$ of 8×10^{-19} zero magnitude, $sec^4/g\text{-}cm^3$ for the Trailblazer Ig artificial meteoroid. Equations (A7) and (A2b) of appendix A were used to calculate a value of $\tau_{o,b}$ of 4×10^{-9} sec/cm from McCrosky and Soberman's data. No estimate of error was made by McCrosky and Soberman.

Verniani, in reference 8, found a linear relationship between velocity and τ_b/ρ_m^2 where ρ_m is the density of the meteoroid. Of the 400 meteors used in his calculations there was only one for which there was conclusive evidence that the meteoroid was similar to meteoritic stone. None of the 400 were identified as meteoritic iron. By using a value of ρ_m of 3.4 g/cm^3 for the stone meteoroid, Verniani reports that $\log \tau'_{o,b} = -19.09 \pm 0.08$, which corresponds to a value of $\tau'_{o,b}$ of $8.1\ (\pm 1.2) \times 10^{-20}$ $sec^4/g\text{-}cm^3$ and a value of $\tau_{o,b}$ of $4.0\ (\pm 0.6) \times 10^{-10}$ sec/cm for stone.

Figure 11 shows that the values for τ_p from the two Trailblazer experiments agree within the limits of experimental error if the same error estimate is applied to both experiments. The values for τ_b (curve III) are about one-half the values for τ_p (curve II) from the same experiment. This difference can be attributed to the difference in the spectral sensitivity of the

I. $\tau_p = \left(1 \times 10^{-8}\right)V$ for stainless steel, from Trailblazer IIb experiment

II. $\tau_p = \left(7 \times 10^{-9}\right)V$ for stainless steel, calculated from Trailblazer Ig data from reference 14

III. $\tau_b = \left(4 \times 10^{-9}\right)V$ for stainless steel, calculated from Trailblazer Ig data from reference 10

IV. $\tau_b = \left(4 \times 10^{-10}\right)V$ for a stone meteoroid, calculated from observational data from reference 8

$\overset{+}{-}$ indicates error estimate

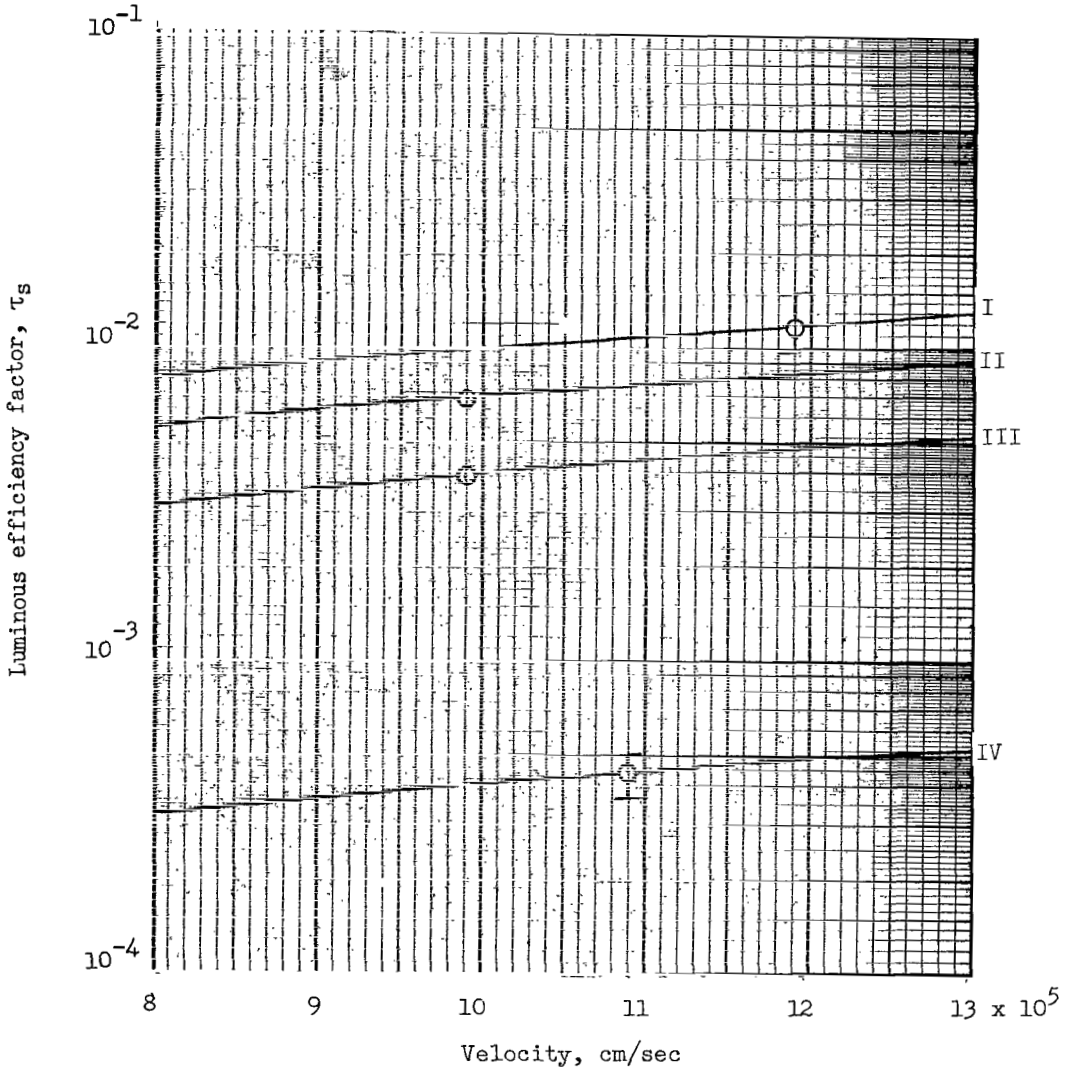

Figure 11.- Comparison of experimental results from two experiments for the luminous efficiency of a stainless-steel artificial meteoroid and observational values for a stone meteoroid.

detectors. The values of τ_b (curve IV) for stone are one-tenth the corresponding values of τ_b (curve III) for stainless steel; this difference can be explained if most of the radiation comes from iron emission from each of the meteoroids. (See ref. 8.)

There is no direct comparison between the values for τ_p or τ_b obtained from the experiments and Öpik's theoretical estimates of the luminous efficiency factor which are in terms of τ_v. In order to make a comparison between the observational data and the theoretical data, a color index must be brought into the calculations. A color index is historically defined as the difference between the photographic (blue sensitive) magnitude and the visual magnitude of an astronomical object. The definition can be extended to mean the difference in magnitude determined by any two detectors. Equations (A8a), (A8b), and (A8c) in appendix A state the needed relationships between values of $\tau'_{o,s}$ derived from different detectors in terms of the color index for the detectors. Given a value of τ_s from one detector, a value of τ_s for another detector can be computed if the color index and the quantity $P_{o,s}$ are adequately known. Appropriate color indexes were applied to the artificial meteoroid data, and the results are shown in figure 12. A smooth curve representation of τ_v for a 2-gram iron meteoroid from Öpik's 1958 theoretical estimates has also been included for comparison.

The value for $\tau'_{o,b}$ from the Trailblazer Ig experiment (ref. 10) was converted to a value of $\tau'_{o,p}$ by use of equation (A8c) of appendix A and average values of M_b and M_p of 0.1 and -0.1, respectively, taken from the published light curves for the meteor. The values of $P_{o,b}$ and $P_{o,p}$ were taken from equations (A2b) and (A2c), and the equation $\tau_p = \tau_{o,p}V$ was used to complete the conversion. The derived value of τ_p of 7.5×10^{-3} at 9.8 km/sec is in excellent agreement with the value of τ_p of 6.8×10^{-3} calculated from the panchromatic data from reference 14.

A visual magnitude for the artificial meteor was not available for either test, and so equations (A9) and (A10) were employed to compute a color index. The value for τ_v computed from τ_b (from ref. 10) and a color index of -1.27 from equation (A9) was an order of magnitude larger than the value for τ_v computed from τ_p (from ref. 14) and a color index of -3.7 from equation (A10). These results from the Trailblazer Ig experiment indicate that the color index equations based on natural meteor observations are not applicable to artificial meteors of the material tested. Without an adequate value for the color index, an accurate comparison between the experimental results and existing theory cannot be made.

I τ_v for a 2-gram iron meteoroid, calculated from Öpik's 1958 theory (ref. 6)

○ τ_p for stainless steel from Trailblazer IIb experiment

□ τ_p for stainless steel, calculated from value of $\tau'_{o,b}$ from Trailblazer Ig data (ref. 10)

◇ τ_p for stainless steel, calculated from value of $\tau_{o,v}$ from Trailblazer Ig data (ref. 14)

△ τ_b for stainless steel, calculated from value of $\tau'_{o,b}$ from Trailblazer Ig data (ref. 10)

◿ τ_v for stainless steel, calculated from value of τ_b (symbol △) using photographic color index

◿ τ_v for stainless steel, calculated from value of τ_p (symbol ◇) using panchromatic color index

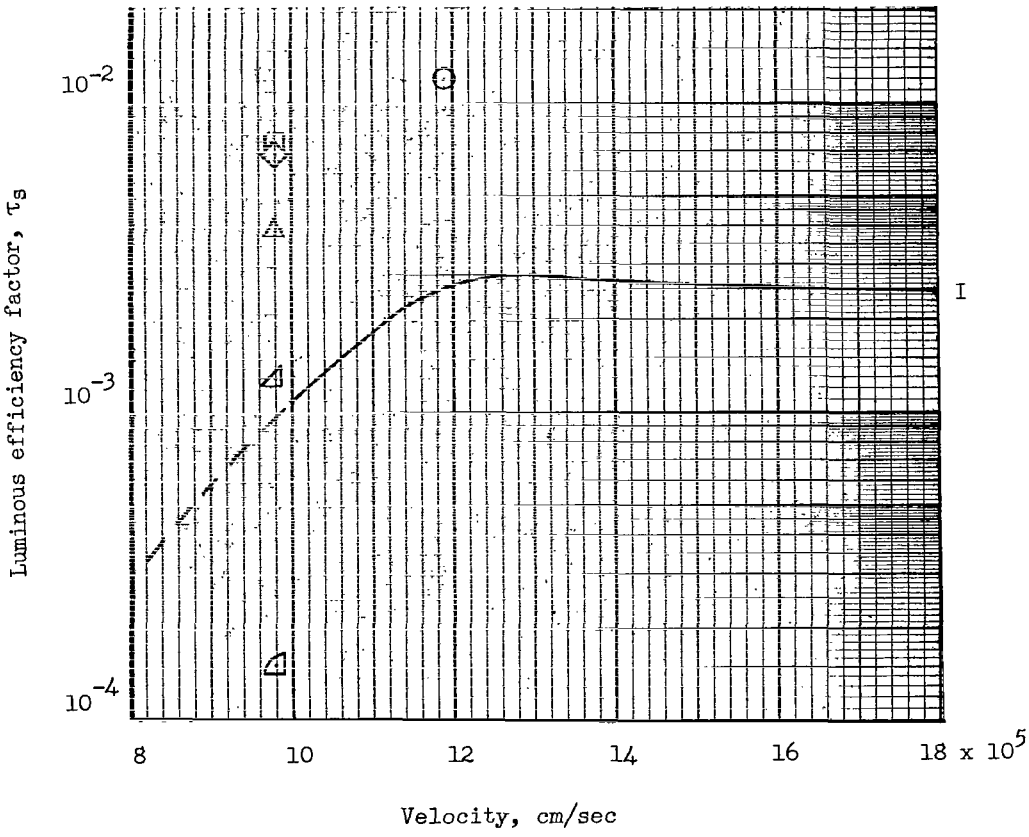

Figure 12.- Effects of spectral response of detectors on measurements of the luminous efficiency factor.

CONCLUDING REMARKS

The Trailblazer IIb experiment was a successful attempt to reenter a 2.2-gram stainless-steel pellet at meteor heights and at the velocity (11.9 km/sec) of a natural meteoroid. By using techniques developed for natural meteors, the photographic data were analyzed and a panchromatic luminous efficiency factor of 1.2×10^{-2} was computed for the artificial meteor. This value for the panchromatic luminous efficiency factor was in good agreement with values obtained from a similar experiment at a lower velocity (9.8 km/sec). An accurate comparison between the panchromatic luminous efficiency factor and theoretical estimates in terms of the visual luminous efficiency factor was not possible because no reliable value for a color index for the meteor was available. It was demonstrated that values for the color index based on natural meteor data gave values for the visual luminous efficiency factor which differed by an order of magnitude.

The comparison of photographic experimental results with the visual theoretical results is somewhat academic since the most accurate data on meteors is now obtained by photography. Meteoroid masses computed from photographic data would be on the basis of a photographic luminous efficiency factor rather than a visual luminous efficiency factor. If experiment and theory are to be accurately compared, either the spectral sensitivity of the detectors should be adjusted to match that of the theoretical detector (the dark adapted eye) or, preferably, the theory should be reworked in terms of modern detectors.

It should be noted at this point that the experimental evidence from artificial meteors is yet too meager to deduce very much about the variation of luminous efficiency with velocity. Several experiments over a wide velocity range would be necessary to do this.

Langley Research Center,
National Aeronautics and Space Administration,
Langley Station, Hampton, Va., April 28, 1965.

APPENDIX A

UNITS AND CONVERSION FORMULAS

Much of the literature concerned with meteor physics contains physical quantities and units which may be unfamiliar to those not working in the field. The purpose of the following discussion is to present those quantities pertinent to the main body of this report and to develop some of the relationships between them.

If the radiant flux and kinetic power in equation (2) are expressed in the same units, that is, ergs/sec or watts, then the luminous efficiency factor τ_s is a dimensionless quantity. However, the radiant flux from a meteor is usually determined by comparison with reference stars which are on a magnitude scale. The primary measure of the radiant power of a meteor, then, is its apparent stellar magnitude. The absolute magnitude M_s of a meteor is defined as the apparent stellar magnitude of the meteor if the meteor were to appear at 100 kilometers and at the zenith. The relationship between the effective radiant power of a meteor and its absolute meteor magnitude can be given by the equation

$$P_s = P_{o,s} 10^{-0.4 M_s} \tag{A1}$$

The quantity $P_{o,s}$ in equation (A1) is the effective radiant power produced by a zero-magnitude meteor. Values for the effective radiant power of a zero-magnitude meteor have been given by Öpik in reference 3 for the visual scale, by Davis and Hall in reference 15 for the photographic scale, and in appendix C of this report for the panchromatic scale. These values are

$$P_{o,v} = 5.26 \times 10^9 \text{ ergs/sec} \tag{A2a}$$

$$P_{o,b} = 5 \times 10^9 \text{ ergs/sec} \tag{A2b}$$

$$P_{o,p} = 7.96 \times 10^9 \text{ ergs/sec} \tag{A2c}$$

Some investigators have chosen to present their results without resorting to conversion factors such as those in equations (A2a), (A2b), and (A2c). Jacchia in reference 7 presents his data in terms of a luminosity factor, McCrosky and Soberman in reference 10 report a value for a luminosity coefficient, and Jewell and Wineman in reference 14 report a value for a luminosity coefficient and also a luminous efficiency factor. Each of these quantities is not only numerically different but is dimensionally different, including the two luminosity coefficients reported in references 10 and 14. The following will be an attempt to present the relationships between these quantities.

APPENDIX A

Jacchia and Whipple in reference 2 noted that Öpik's 1933 data on the visual luminous efficiency factor τ_V for bright meteors (curve I in fig. 2(a)) could be represented by an equation of the form

$$\tau_V = \tau_{0,V} V \tag{A3}$$

The multiplying factor $\tau_{0,V}$ was termed the luminosity coefficient and had a numerical value of 8.5×10^{-10} sec/cm. According to reference 1, p. 175, the relationship given by equation (A3) ". . . is applicable to the brighter photographic meteors only, and even in these cases its validity is now regarded skeptically."

Jacchia in reference 7 writes the luminosity equation as

$$M_V = M_0 - 2.5 \log\left(-\frac{dm}{dt}\right) - 7.5 \log V \tag{A4}$$

and designates M_0 as the luminosity factor. An equation of the same form as equation (A4) may be obtained by substituting equations (A1) and (A3) into equation (2) and writing the resulting equation logarithmically to obtain

$$M_s = 2.5 \log P_{0,s} - 2.5 \log \frac{\tau_{0,s}}{2} - 2.5 \log\left(-\frac{dm}{dt}\right) - 7.5 \log V \tag{A5}$$

A comparison of equations (A5) and (A4) shows that the relationship between the luminosity factor and the luminosity coefficient is evidently

$$M_0 = -2.5 \log \frac{\tau_{0,s}}{2P_{0,s}} \tag{A6}$$

McCrosky and Soberman in reference 10 use an equation of the same form as equation (2) but take $P_{0,s}$ as the unit of power (i.e., $P_{0,s} = 1$). If the luminosity coefficient from reference 10 is designated as $\tau'_{0,s}$ and the luminosity coefficient from reference 14 is designated as $\tau_{0,s}$, the relationship between the quantities is

$$\tau_{0,s} = P_{0,s} \tau'_{0,s} \tag{A7}$$

with $\tau_{0,s}$ having the unit of sec/cm and $\tau'_{0,s}$ having the unit of $sec^4/g\text{-}cm^3$ for the cgs system of units.

Even if the quantities reported were dimensionally the same, a direct comparison cannot be made between quantities from different sources unless they are based on similar detection systems. However, conversion formulas for quantities from the different detection systems may be developed.

APPENDIX A

The following relationships are derived from equation (A5):

$$\log \frac{\tau_{o,v}}{P_{o,v}} = \log \frac{\tau_{o,b}}{P_{o,b}} + 0.4\left(M_b - M_v\right) \tag{A8a}$$

$$\log \frac{\tau_{o,v}}{P_{o,v}} = \log \frac{\tau_{o,p}}{P_{o,p}} + 0.4\left(M_p - M_v\right) \tag{A8b}$$

$$\log \frac{\tau_{o,p}}{P_{o,p}} = \log \frac{\tau_{o,b}}{P_{o,b}} + 0.4\left(M_b - M_p\right) \tag{A8c}$$

These equations can be used to calculate the visual luminosity coefficient if the terms within parentheses are adequately known. The term $M_b - M_v$ is known as the color index C_b. Jacchia (ref. 16) has found a dependence of the color index on the brightness of meteors but no dependence on velocity. There is no distinction made between meteoroids of different composition. Jacchia's results may be summarized by the equations

$$\left.\begin{aligned} C_b &= 0.3M_b - 1.3 \qquad \text{for } -2 < M_b < 1.5 \\ C_b &= -1.9 \qquad\qquad\quad \text{for } -5 < M_b < -2 \end{aligned}\right\} \tag{A9}$$

Ceplecha, as reported by Davis in reference 17, has found a similar relationship for the panchromatic color index, which is $C_p = M_p - M_v$. His results may be summarized by the equations

$$\left.\begin{aligned} C_p &= -0.6M_p - 5.2 \qquad \text{for } -4.5 < M_p < -2.5 \\ C_p &= -3.7 \qquad\qquad\quad\;\; \text{for } -2.5 < M_p \end{aligned}\right\} \tag{A10}$$

It should be noted that the blue sensitive color index C_b and the panchromatic color index C_p vary with magnitude in an opposite sense; that is, C_b increases for faint meteors whereas C_p increases for bright meteors. This would indicate that the predominate radiation from bright meteors is at longer wavelengths than radiation from fainter meteors. The large differences in panchromatic, blue sensitive, and visual meteor magnitudes as implied by equations (A9) and (A10) are also of considerable interest, since these differences in magnitude would reflect in large differences in values of τ_s, depending on the detection system that is used.

APPENDIX B

CORRESPONDENCE BETWEEN PANCHROMATIC AND VISUAL MAGNITUDES

The earliest photographic emulsions were sensitive only to the blue portion of the spectrum. Consequently, the term photographic magnitude usually refers to stellar magnitudes determined from blue sensitive plates. It has been found experimentally that stellar magnitudes determined from the panchromatic records are closer approximations to the visual magnitudes of the stars than to their photographic magnitudes.

Figure 13(a) is a plot of the optical density of a number of star images measured from one panchromatic photographic plate against the photographic magnitudes from reference 13. Figure 13(b) is a plot of the same density readings against the visual magnitudes from reference 13. The different symbols identify the stars by spectral class.

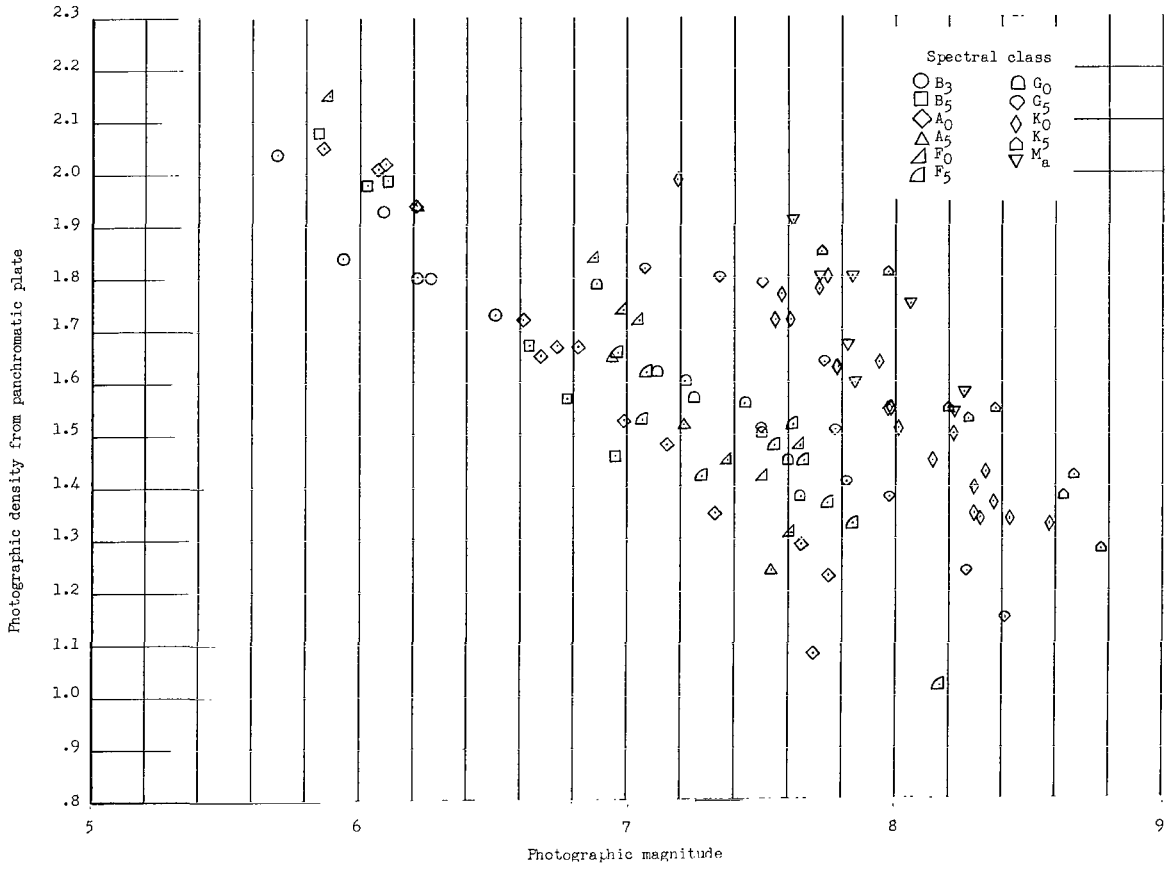

(a) Variation with photographic magnitude of stars.

Figure 13.- Photographic density from a panchromatic plate of the stellar images.

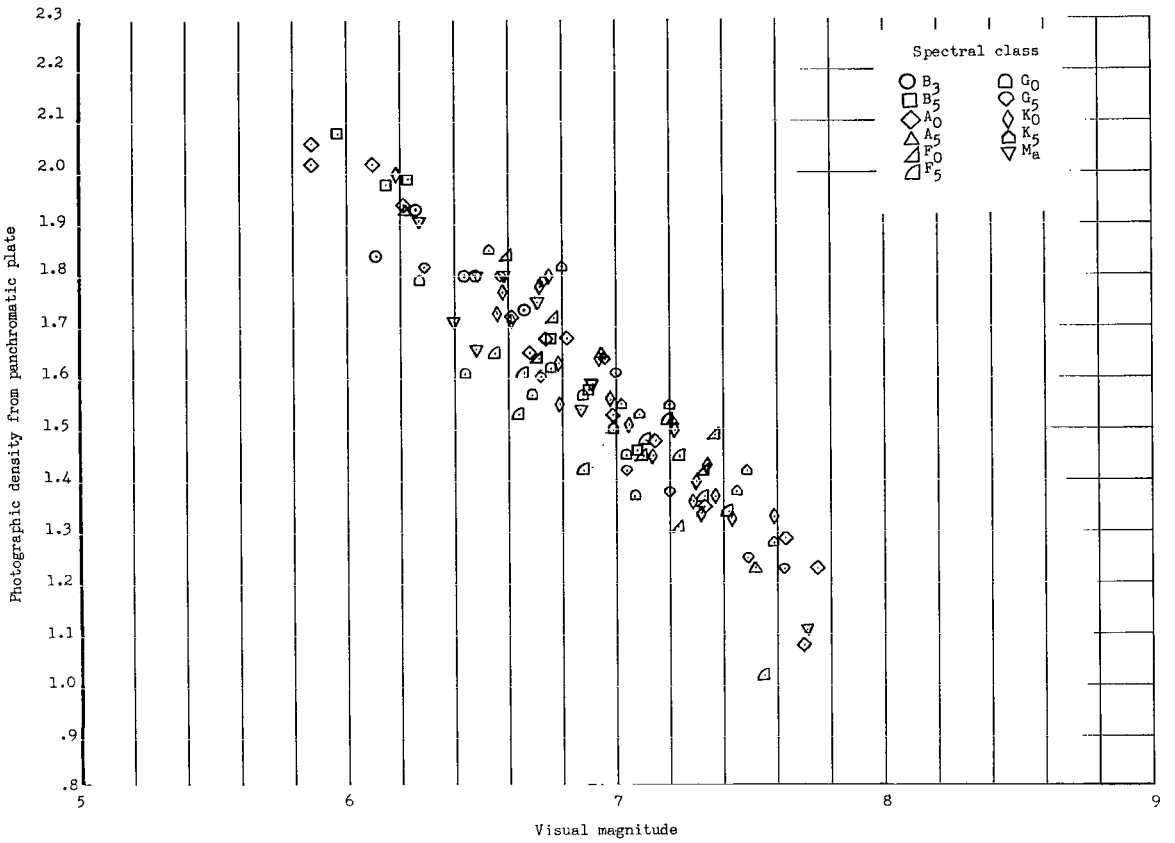

(b) Variation with visual magnitude of stars.

Figure 13.- Concluded.

The spread in the points along the magnitude axis is a measure of the difference between the panchromatic magnitudes and the photographic or visual magnitudes. In figure 13(a) the spread is approximately 2.0 magnitudes, and there is a separation by spectral class. The blue stars group at one edge and redder stars are found near the other side of the distribution. When the measured densities are plotted against visual magnitude (fig. 13(b)), the spread is decreased to approximately 0.8 magnitude, and there is no apparent separation by the spectral class.

An attempt was made to obtain quantitative information for the data presented in figure 13. A curve of the form $M_V = a + bD$ was fitted by least squares to the visual magnitudes M_V of the A_0 stars given in reference 13 and their measured densities D. This equation was then used as the defining equation for a panchromatic magnitude scale for all the stars in the set; that is, $M_p = a + bD$ for all stars of the set with the constants a and b having the values determined by least squares for the A_0 stars. The panchromatic magnitude M_p for each star was determined. The average panchromatic color index

for each spectral class of stars was then determined from the equation

$$\overline{C}_p = \sum \frac{M_p - M_v}{n}$$

and is presented in table III along with the color index, $C_b = M_b - M_v$, that is used in reference 13.

TABLE III.- COLOR INDEX FOR STARS

Spectral class	Number of stars used	Average panchromatic color index, $\overline{C}_p$	Standard deviation of C_p	Blue sensitive color index from ref. 13, C_b
B_3	5	-0.07	0.20	-0.17
B_5	6	.02	.06	-.12
A_0	14	.00	.09	.00
A_5	4	.07	.10	.14
F_0	7	.04	.14	.23
F_5	10	.14	.21	.42
G_0	8	.19	.12	.56
G_5	10	.00	.15	.78
K_0	20	.05	.10	1.00
K_5	8	.16	.10	1.18
M_a	9	.08	.13	1.35

It should be noted that the standard deviation is generally greater than the average value of C_p. This indicates that the difference between visual magnitudes and panchromatic magnitudes within any one spectral class is as great as the magnitude difference between stars of different spectral classes when this method of photometry is used.

Although the panchromatic emulsion gives stellar magnitudes close to visual magnitudes, the results cannot be extrapolated to meteor magnitudes. Stellar radiation is essentially continuous whereas bright lines characterize meteor radiation. This difference in the quality of radiation may very well result in a large difference in the visual magnitude and panchromatic magnitude for meteors.

APPENDIX C

RELATIONSHIP BETWEEN THE PANCHROMATIC MAGNITUDE AND EFFECTIVE RADIANT POWER OF A METEOR

A comparison of the meteor trail with a set of reference stars gives a measure of the irradiance from the meteor at the point of observation. The relationship between irradiance and stellar magnitudes may be given as

$$M_s - M_{ref} = -2.5 \log \frac{H_s}{H_{ref}} \tag{C1}$$

where the subscript ref indicates a reference source that sets the zero of the magnitude scale.

The effective irradiance H_s is given by

$$H_s = \int_0^\infty S_\lambda H_\lambda \, d\lambda \tag{C2}$$

where S_λ is the spectral sensitivity function for the detector, H_λ is the spectral irradiance due to the source, and λ is the wavelength.

The purpose of the following calculation is to relate the absolute panchromatic magnitude of a meteor to the effective radiant power produced by the meteor. The effective radiant power P_s of a point source which will produce an irradiance H_s at 100 kilometers from the source is

$$P_s = \left(4\pi \times 10^{14}\right) H_s \text{ ergs/sec} \tag{C3}$$

when H_s is expressed in ergs/cm^2-sec. The sun is a convenient astronomical object for which values of H_λ are readily available. If values for H_λ from reference 18 are used and the spectral sensitivity function for a panchromatic detector represented by figure 1(c) is used, the effective panchromatic irradiance of the sun will be

$$H_{p,sun} = \int_0^\infty S_p H_{\lambda,sun} \, d\lambda = 3.1 \times 10^5 \text{ ergs/cm}^2\text{-sec}$$

The effective panchromatic radiant power of a point source which will produce an irradiance at 100 kilometers equal to the sun irradiance at one astronomical unit is simply

$$P_{p,100} = 3.9 \times 10^{20} \text{ ergs/sec} \tag{C4}$$

The stellar magnitude of a point source at 100 kilometers that matches the solar irradiance will have an apparent magnitude equal to that of the sun. By taking the solar panchromatic magnitude to be equal to the solar visual magnitude (see appendix B) and the value of the effective radiant power computed for a point source at 100 kilometers, an absolute meteor magnitude scale for panchromatic detectors may be given in terms of effective power as

$$M_p + 26.72 = -2.5 \log \frac{P_p}{3.9 \times 10^{20}} \tag{C5}$$

which reduces to

$$M_p = 24.76 - 2.5 \log P_p \tag{C6}$$

The value -26.72 for the visual magnitude of the sun is taken from reference 3. From equation (C6), a zero-magnitude meteor will produce 7.96×10^9 ergs/sec of power capable of producing a response in a panchromatic detector, or

$$P_{o,p} = 7.96 \times 10^9 \text{ ergs/sec} \tag{C7}$$

REFERENCES

1. McKinley, D. W. R.: Meteor Science and Engineering. McGraw-Hill Book Co., Inc., 1961.

2. Jacchia, Luigi G.; and Whipple, Fred L.: The Harvard Photographic Meteor Programme. Vol. 2 of Vistas in Astronomy, A. Beer, ed., Pergamon Press, 1956, pp. 982-994.

3. Öpik, Ernst J.: Physics of Meteor Flight in the Atmosphere. Interscience Publ., Inc. (New York), 1958.

4. Anon.: Kodak Plates and Films for Science and Industry. Publ. No. P-9, Eastman Kodak Co., 1962.

5. Anon.: Kodak Royal-X Pan Recording Film. Pamphlet No. P-38, Eastman Kodak Co.

6. Öpik, Ernst: Atomic Collisions and Radiation of Meteors. Reprint 100, Harvard Univ. (From Acta et Commentationes Universitatis Tartuensis (Dorpatensis) A XXVI.2, 1933.)

7. Jacchia, Luigi G.: Photographic Meteor Phenomena and Theory. Tech. Rept. No. Three (Contracts NOrd 8555 and 10455), Harvard College Observatory and Center of Analysis, M.I.T., 1949.

8. Verniani, Franco: On the Luminous Efficiency of Meteors. Spec. Rept. No. 145, Smithsonian Inst. Astrophys. Obs., Feb. 17, 1964.

9. Middlehurst, Barbara M.; and Kuiper, Gerard P., eds.: The Moon, Meteorites, and Comets. The Univ. Chicago Press, c.1963.

10. McCrosky, Richard E.; and Soberman, Robert K.: Results From an Artificial Iron Meteoroid at 10 km/sec. AFCRL-62-803, U.S. Air Force, July 1962.

11. Lundstrom, Reginald R.; Henning, Allen B.; and Hook, W. Ray: Description and Performance of Three Trailblazer II Reentry Research Vehicles. NASA TN D-1866, 1964.

12. Whipple, Fred L.; and Jacchia, Luigi G.: Reduction Methods for Photographic Meteor Trails. Smithsonian Contributions to Astrophysics, vol. 1, no. 2, 1957, pp. 183-206.

13. Cannon, Annie J.; and Pickering, Edward C.: The Henry Draper Catalogue. Vols. 91-99 of Annals of the Astronomical Observatory of Harvard College, 1918-1924.

14. Jewell, W. O.; and Wineman, A. R.: Preliminary Analysis of a Simulated Meteor Reentry at 9.8 Kilometers per Second. NASA TN D-2268, 1964.

15. Davis, J.; and Hall, J. E.: Meteor Luminosity and Ionization. Proc. Roy. Soc. (London), ser. A, vol. 271, no. 344, Jan. 1, 1963, pp. 120-128.

16. Jacchia, L. G.: On the "Color Index" of Meteors. The Astronomical J., vol. 62, no. 1254, Dec. 1957, pp. 358-362.

17. Davis, John: Photoelectric Meteor Observations and the Colour Indices and Visual Magnitudes of Meteors. Monthly Notices, Roy. Astron. Soc., vol. 126, no. 5, 1963, pp. 445-467.

18. Anon.: Handbook of Geophysics. Revised ed., The Macmillan Co., 1961.

NASA-Langley, 1965 L-4387

2/22/85
OB

"The aeronautical and space activities of the United States shall be conducted so as to contribute . . . to the expansion of human knowledge of phenomena in the atmosphere and space. The Administration shall provide for the widest practicable and appropriate dissemination of information concerning its activities and the results thereof."

—NATIONAL AERONAUTICS AND SPACE ACT OF 1958

NASA SCIENTIFIC AND TECHNICAL PUBLICATIONS

TECHNICAL REPORTS: Scientific and technical information considered important, complete, and a lasting contribution to existing knowledge.

TECHNICAL NOTES: Information less broad in scope but nevertheless of importance as a contribution to existing knowledge.

TECHNICAL MEMORANDUMS: Information receiving limited distribution because of preliminary data, security classification, or other reasons.

CONTRACTOR REPORTS: Technical information generated in connection with a NASA contract or grant and released under NASA auspices.

TECHNICAL TRANSLATIONS: Information published in a foreign language considered to merit NASA distribution in English.

TECHNICAL REPRINTS: Information derived from NASA activities and initially published in the form of journal articles.

SPECIAL PUBLICATIONS: Information derived from or of value to NASA activities but not necessarily reporting the results of individual NASA-programmed scientific efforts. Publications include conference proceedings, monographs, data compilations, handbooks, sourcebooks, and special bibliographies.

Details on the availability of these publications may be obtained from:

SCIENTIFIC AND TECHNICAL INFORMATION DIVISION

NATIONAL AERONAUTICS AND SPACE ADMINISTRATION

Washington, D.C. 20546